

SYNCHRONIZATION MEASURES OF THE SCALP ELECTROENCEPHALOGRAM CAN DISCRIMINATE HEALTHY FROM ALZHEIMER'S SUBJECTS

MARK A. KRAMER*

*Graduate Group in Applied Science and Technology,
University of California, Berkeley, Berkeley, CA, USA*

FEN-LEI CHANG

*Indiana University School of Medicine — Fort Wayne,
Fort Wayne, IN, 46805, USA*

MAURICE E. COHEN

*Department of Radiology,
UCSF-Fresno, Fresno, CA, USA*

DONNA HUDSON

*Family and Community Medicine,
UCSF-Fresno, Fresno, CA, USA*

ANDREW J. SZERI†

*Department of Mechanical Engineering,
Graduate Group in Applied Science and Technology,
University of California, Berkeley, Berkeley, CA, USA
andrew.szeri@berkeley.edu*

Three synchronization measures are applied to scalp electroencephalogram (EEG) data collected from 20 patients diagnosed to have either: (1) no dementia, (2) mild cognitive impairment (MCI), or (3) Alzheimer's disease (AD). We apply the three synchronization measures — the phase synchronization, and two measures of nonlinear interdependency — to the data collected from awake patients resting with eyes closed. We show that the synchronization in potential between electrodes near the left and right occipital lobes provides a statistically significant discriminant between the healthy and AD subjects, and the MCI and AD subjects. None of the three measures appears able to distinguish between the healthy and MCI subjects, although MCI subjects show synchronization values intermediate between healthy subjects (with high synchronization values) and AD subjects (with low synchronization values) on average.

Keywords:

1. Introduction

The most common form of dementia, Alzheimer's disease (AD), affects 4.5 million people in the U.S.¹ At present, no cure for AD exists, although some medications may delay memory decline or treat behavioral and emotional symptoms.² The primary treatment for AD is supportive care provided both

to patients and their families. In 1991, the costs of treating AD in America were estimated to exceed 67 billion dollars, and are expected to increase dramatically during the next 25 years.³

Although prevalent, AD is difficult to diagnose. The gold standard for diagnosis occurs post-mortem when an autopsy reveals neurofibrillary tangles or

*Present address: Center for BioDynamics, Boston University, 111 Cummington Street, Boston, MA, 02215, USA.

†Corresponding author.

amyloid plaques in the cortex and hippocampus. The clinical diagnosis of AD is often accurate (in greater than 80% of cases), yet the similarity of symptoms expressed in AD and other forms of dementia and depression often hinders the diagnosis.⁴ In addition, physicians must diagnose patients intermediate between cognitively normal elderly individuals and those with dementia.² This intermediate zone is referred to as mild cognitive impairment (MCI) and patients diagnosed with MCI are 5 to 10 times more likely to develop dementia.² That MCI symptoms often precede AD suggests the possibility of detecting AD before its complete onset. Early detection of AD would provide individuals more time to make special arrangements and perhaps allow future preventative treatments to be administered.

The scalp electroencephalogram (EEG) reveals changes in cortical electrical activity associated with normal aging, MCI, and AD. The most established of these EEG diagnostic techniques analyze changes in the power spectrum. Many researchers have found that AD patients exhibit increased power in the δ ($\approx 1 - 3$ Hz) and θ ($\approx 4 - 7$ Hz) frequency bands, and decreased power in the α ($\approx 8 - 12$ Hz) and β ($\approx 13 - 28$ Hz) frequency bands compared to healthy controls.⁴⁻⁶ This “slowing” of the EEG occurs across the scalp with a nearly uniform spatial distribution. Recently, researchers have shown that measures adopted from dynamical systems theory, such as the correlation dimension, reveal decreased complexity of EEG traces from AD patients.^{7,8}

Both the power spectrum and correlation dimension are computed from EEG data collected at individual electrodes. Thus, these two measures reveal changes in the spatially localized voltage produced near each electrode. Coupling measures, on the other hand, reveal changes in the interdependence of EEG data recorded at two different electrodes. For example, linear coherence is a frequency-domain measure of coupling between two time series. Researchers have applied linear coherence measures to EEG data and found that patients diagnosed with AD often exhibit a lower coherence between electrode pairs than healthy controls.⁹ These decreased coherence values are typically localized in both frequency and location (e.g., decreased frontal cortex coupling and central cortex coupling in the θ , α , and β bands,¹⁰ decreased temporofrontal coupling and temporoparietal coupling in the α band,⁶ decreased temporal

lobe coupling in the α band.¹¹) Recently, measures of nonlinear coupling between two time series have been developed.¹²⁻¹⁵ In Ref. 16 the authors apply one of these measures to EEG data collected from healthy, MCI, and AD subjects. They find that cortical interactions in AD patients decrease in the β band compared to healthy controls.

Here we study resting scalp EEG collected from 20 individuals clinically diagnosed to have either no dementia (7 healthy controls, ages 62 ± 14 years, we denote as N), MCI (5 subjects, ages 71 ± 5 years), or AD (8 subjects, ages 81 ± 6 years.) In Sec. 2 we discuss the clinical diagnosis of these conditions and the data collection procedure, and in Sec. 3 we describe three synchronization measures in common use. We apply the synchronization measures to the EEG data in Sec. 4 and show that the synchronization between EEG time series recorded at electrodes O1 and O2 — above the left and right occipital lobes, respectively — provides a quantitative means to discriminate AD subjects from healthy and MCI subjects. In Sec. 5 we discuss how these synchronization results suggest changes in neural connectivity.

2. Clinical Diagnosis and Data Collection

Each subject was assigned a clinical diagnosis by a team of physicians at the Fort Wayne Neurological Center in Fort Wayne, Indiana. These diagnoses were based on a medical history, a neurocognitive history, neurological examination, neuropsychological tests, brain images, and blood tests. As part of the assessment, scalp EEG data were collected from each subject. These data were recorded using the standard 10-20 electrode configuration with a linked-ears reference and a sampling rate of 256 Hz. During the data collection, typically lasting 30 minutes, each subject was instructed to relax and close his or her eyes. Deviations from this behavior, such as eye movements or sleep, were noted and the associated time intervals were omitted from further analysis. In what follows we analyze these EEG data in accordance with human subjects guidelines established by the University of California, Berkeley. Research protocol were approved by the University of California, San Francisco and the Parkview Hospital IRB at Fort Wayne, Indiana.

3. Methods

The goal of the analysis is to provide a concise, quantitative measure capable of distinguishing between AD, MCI, and healthy subjects from the scalp EEG data. To do so, we apply three synchronization measures to the EEG data and determine the nonlinear coupling between time series recorded at two, neighboring electrodes. In this section, we describe the preprocessing of the data and the additional processing we perform on the results of the three synchronization measures. We apply these measures to the data in Sec. 4.

We start the analysis by choosing two neighboring electrodes (O1 and O2, say) from one subject. For convenience, we label the time series recorded at the two electrodes $x[t]$ and $y[t]$ where $t = \{0, \dots, T\}$ is the time index, and T is the total number of data points collected. We note that to derive the time (in seconds) from the time index, we multiply t by the sampling interval 1/256 s. The preprocessing of $x[t]$ and $y[t]$ consists of three steps. First, we average reference the data with respect to the remaining 19 electrodes; for one subject, we computed the average reference over 18 electrodes because the voltage at the omitted 19th electrode reached saturation. We note that — in the unprocessed data — the linked-ears reference electrodes act as a common signal added to each channel and may induce an artificial increase in the coupling results. To avoid this, we compute the average reference of the data as a crude approximation of reference-independent voltages.¹⁷ Second, we bandpass digital filter the data between 1 Hz and 50 Hz, subtract the mean from each electrode, and scale the data to have a maximum absolute value of one. Third, we divide $x[t]$ and $y[t]$ into 120, consecutive, one second intervals (256 index points per interval). We choose these intervals from simultaneous segments of $x[t]$ and $y[t]$. For example, if we choose the first segment in $x[t]$ from $256 \leq t \leq 511$, then the first segment in $y[t]$ is from $256 \leq t \leq 511$. We label the data in each interval chosen in this way from $x[t]$ and $y[t]$ as $x^i[t]$ and $y^i[t]$, respectively. We note that the superscript i denotes the i^{th} interval. Finally, we label the data from $x[t]$ and $y[t]$ referenced, filtered, with fixed mean, scaled, and divided into intervals, as $\tilde{x}^i[t]$ and $\tilde{y}^i[t]$, respectively. In this way, we create an ensemble of measurements.

To determine the coupling between the ensembles $\tilde{x}^i[t]$ and $\tilde{y}^i[t]$ we apply three different synchronization measures. These synchronization measures are recent algorithms adapted from dynamical systems theory. The advantage of synchronization measures over traditional techniques of time series analysis (such as the linear coherence results in Refs. 6, 9, 10 and 11) is that synchronization measures detect nonlinear coupling between two time series. A measure of nonlinear interdependence may be especially important when studying complicated systems, such as the human neocortex. It is reasonable to assume that, because of the nonlinear processing of single neurons and the high density of cortical connections, the EEG does possess a nonlinear component (i.e., the EEG cannot be modeled only as a collection of independent oscillators or modes.¹⁸) To apply these ideas, we must also assume that the EEG is the result of a low dimensional, deterministic process.¹⁹ Without these assumptions, we may still apply the synchronization measures to characterize the EEG signal. Here we need not interpret the results in terms of low dimensional dynamical systems; instead we apply the synchronization measures to discriminate between the healthy, MCI, and AD subjects.

Before applying the three synchronization measures to the EEG data, we outline how each is computed. Two of the synchronization measures, $S(x|y)$ and $H(x|y)$, are similar and defined in Refs. 13 and 14. To compute $S(x|y)$ or $H(x|y)$, we first delay-time embed the data $\tilde{x}^i[t]$ and $\tilde{y}^i[t]$ from interval i . The embedding procedure creates d -dimensional vectors $\tilde{X}^i[t]$ and $\tilde{Y}^i[t]$ from the 1-dimensional vectors $\tilde{x}^i[t]$ and $\tilde{y}^i[t]$, respectively. For example, we may define the 3-dimensional vector $\tilde{X}^i[t] = \{\tilde{x}^i[t], \tilde{x}^i[t + \tau], \tilde{x}^i[t + 2\tau]\}$. Here $\tilde{X}^i[t]$ is expressed in terms of $\tilde{x}^i[t]$ and the value of $\tilde{x}^i[t]$ shifted by time τ . There exist procedures to choose the dimension d and delay-time τ for noise-free data.²¹ We do not apply these procedures here; instead, we choose different values of d and τ and show that the results are invariant. In Refs. 7 and 8, the authors follow a similar procedure and compute the correlation dimension for different values of d and τ .

After embedding the data in interval i , we compute the synchronization measures $S(x|y)$ and $H(x|y)$ by determining neighborhoods in $\tilde{X}^i[t]$ and

4 *M. A. Kramer et al.*

$\tilde{y}^i[t]$ in the higher-dimensional space. To define the neighborhood of $\tilde{Y}^i[t]$ at $t = 0$, say, we locate the points in $\tilde{Y}^i[t]$ nearest to $\tilde{Y}^i[0]$. Here nearness is measured in terms of the Euclidean distance. We identify the 30 points closest to $\tilde{Y}^i[0]$ by their indices; for example, let $t \in \{11, 130, 145, \dots\}$ index the 30 points closest to $\tilde{Y}^i[0]$. To avoid serial correlations in the data, we choose neighbors to lie outside a temporal window of size 10 (approximately 40 ms) around $t = 0$. Therefore the point $\tilde{Y}^i[1]$ is not considered as a neighbor of $\tilde{Y}^i[0]$ no matter how close in the embedded space these two points may be. Now we consider the vector $\tilde{X}^i[t]$ at $t = 0$, and compute the distance from $\tilde{X}^i[0]$ to $\tilde{X}^i[t]$ with indices $t \in \{11, 130, 145, \dots\}$. In this step, we use the time indices from $\tilde{Y}^i[t]$ to compute spatial distances in $\tilde{X}^i[t]$. If these distances are small, then the time indices of neighbors of $\tilde{Y}^i[0]$ also belong to a neighborhood of $\tilde{X}^i[0]$. We then say that $\tilde{Y}^i[0]$ and $\tilde{X}^i[0]$ are synchronous at $t = 0$. This is how neighborhoods in $\tilde{Y}^i[t]$ are compared to neighborhoods in $\tilde{X}^i[t]$, and is the fundamental concept of these two synchronization measures.

The subsequent computation of $S(x|y)$ and $H(x|y)$ that measure the level of this synchronization is similar.^{13,14} Both involve an embedding procedure, a determination of neighborhoods, and a ratio of distances. Synchronization values near 0 represent weak interdependence, while synchronization values near 1 represent strong interdependence. The result of applying these measures to $\tilde{x}^i[t]$ and $\tilde{y}^i[t]$ for each i is the synchronization as a function of time t within interval i . To provide a concise diagnostic measure of dementia, we make two assumptions regarding the stationarity of the synchronization results. First, we assume that within each one second interval i the synchronization between $\tilde{x}^i[t]$ and $\tilde{y}^i[t]$ remains statistically approximately constant. We may then average the synchronization values over time t for fixed i . Second, we assume that the synchronization results are stationary over the 120 intervals, and therefore average the synchronization results across intervals i . Both stationarity assumptions are likely invalid — the neural activity of the neocortex continually evolves in response to input from, for example, environmental stimuli and the thalamus. But, we show below that these assumptions do not prevent the goal of this work: to discriminate between healthy, MCI, and AD subjects. The final result is

two scalar values representing the average $S(x|y)$ and $H(x|y)$ results for each subject.

The third measure we employ is the phase synchronization $P(\theta)$. There exist many definitions of phase synchronization; the one we use here is similar to that stated in Ref. 22. The first step in computing $P(\theta)$ is to apply the Hilbert transform to $\tilde{x}^i[t]$ and $\tilde{y}^i[t]$, and extract the instantaneous phase θ from each as a function of time index t . We then compute the phase difference between $\tilde{x}^i[t]$ and $\tilde{y}^i[t]$ at each t ; this is identical to the 1 : 1 phase locking in Ref. 22. Finally, we define $P(\theta)$ as the probability that the phase difference between $\tilde{x}^i[t]$ and $\tilde{y}^i[t]$ assumes the value θ , where $0 \leq \theta < 2\pi$, during the interval i .²³ We compute $P(\theta)$ between $\tilde{x}^i[t]$ and $\tilde{y}^i[t]$ for all intervals i . To provide a summary measure, we average $P(\theta)$ over all intervals and over phases θ near 0; specifically, we average $P(\theta)$ over phases between 0.0 and 0.3, and between $2\pi - 0.3$ and 2π . Here we again assume the stationarity of the phase synchronization over the intervals. In addition, we consider only the 1 : 1 phase locking at near zero phase. We have found, but do not show, that $P(\theta)$ is unimodal with largest peak near $\theta = 0$ in the data considered here. The final result is a scalar value representing the average $P(\theta)$ for each subject.

4. Results

Having defined the three synchronization measures in common use, we now apply each measure to the EEG data sets recorded from the neural system. We illustrate the results with two examples. First, we apply the three synchronization measures to the EEG data collected at electrodes O1 and O2, located near the left and right occipital lobes, respectively. We show that two measures — $S(x|y)$ and $H(x|y)$ — produce similar results and significant (or near significant) separation between the healthy and AD subjects and the MCI and AD subjects for different embedding parameters d and τ . We note that the measure $P(\theta)$ is independent of the embedding parameters because it is estimated without need of an embedding. Second, for $d = 10$ and $\tau = 1$, we compare the synchronization between electrodes P3 and P4 using each of the measures. In this case, we find no significant separation between the conditions. We find, but do not show, similar insignificant separation between the three subject groups for three

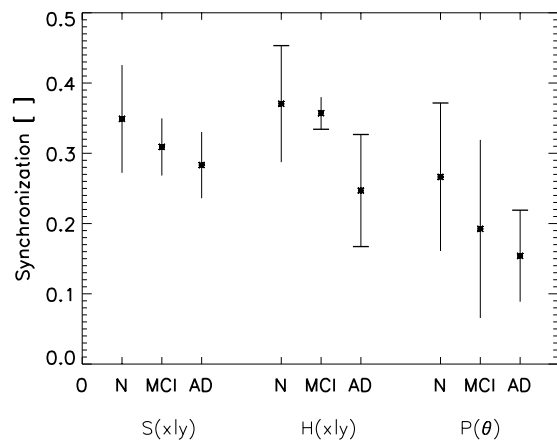


Fig. 1. The synchronization values for the three measures $S(x|y)$, $H(x|y)$, and $P(\theta)$ between electrodes O1 and O2 averaged over the three subject groups: healthy (N), mild cognitive impairment (MCI), and Alzheimer's disease (AD). We plot the results for the three synchronization measures $S(x|y)$, $H(x|y)$, and $P(\theta)$ from left to right, respectively. We indicate the average synchronization values by asterisks and the standard deviation within each subject group by vertical lines extending above and below each asterisk. The synchronization values and standard deviations are also listed in Table 1. We indicate statistically significant ($p < 0.05$) separations between the N and AD values by drawing a small horizontal line one standard deviation *above* the mean synchronization values for the healthy and AD subjects. We indicate statistically significant ($p < 0.05$) separations between the MCI and AD values by drawing a small horizontal line one standard deviation *below* the mean synchronization values for the MCI and AD subjects.

other pairs of interhemispheric electrodes: C3 and C4, F3 and F4, and FP1 and FP2. We conclude that the AD subjects show decreased synchronization between the left and right occipital lobes compared to the healthy and MCI subjects.

We start with the application of the synchronization measures to the EEG data collected at electrodes O1 and O2. We show the results for the embedding parameters $d = 10$ and $\tau = 1$ in Fig. 1. For each of the three synchronization measures ($S(x|y)$, $H(x|y)$, and $P(\theta)$) we plot the results for the three subject groups (N, MCI, and AD). We indicate the mean value for each subject group and condition with an asterisk, and the standard deviation by vertical lines extending above and below each asterisk. We also list the synchronization values and standard deviations in Table 1. We note that the three synchronization measures illustrated in Fig. 1 produce

Table 1. The value and standard deviation of the synchronization between electrodes O1 and O2 averaged over subject groups. We mark the statistically significant separations ($p < 0.05$) between the healthy and AD subjects, and the MCI and AD subjects with an asterisk (*) and double asterisk (**), respectively.

	$S(x y)$	$H(x y)$ [*, **]	$P(\theta)$ [*]
N	0.35 ± 0.08	0.37 ± 0.08	0.27 ± 0.10
MCI	0.31 ± 0.04	0.36 ± 0.02	0.19 ± 0.13
AD	0.28 ± 0.05	0.25 ± 0.08	0.15 ± 0.05

similar results. Specifically, we find that the average synchronization values for the healthy subjects exceeds the average synchronization values for the AD subjects. The separation between these two values is statistically significant (t -means test $p < 0.05$) for two measures: $H(x|y)$ and $P(\theta)$. We indicate this significant separation by drawing a small horizontal line one standard deviation *above* the mean values for the healthy and AD subjects. We note that the separation is near significance ($p = 0.08$) for $S(x|y)$. We also find that the average synchronization for the MCI subjects is less than that of the healthy subjects and greater than that of the AD subjects. These differences are not statistically significant except for the separation between the MCI and AD subjects computed with $H(x|y)$. We indicate this significant separation by drawing a small horizontal line one standard deviation *below* the mean values for the MCI and AD subjects. We note that we find identical trends and statistically significant changes for $S(x|y)$ and $H(x|y)$ if we choose neighborhoods in the embedded space of 20 or 40 points instead of 30 points.

In Fig. 2 we show the synchronization measures $S(x|y)$ and $H(x|y)$ computed with different embedding parameters d . Here we fix $\tau = 1$ and plot the synchronization results for $d = 4$ (in squares and dotted lines,) $d = 10$ (in asterisks and solid lines — as in Fig. 1,) and $d = 16$ (in diamonds and dashed lines.) We find that, compared to the $d = 10$ results, the mean values of $S(x|y)$ decrease for $d = 4$ and increase for $d = 16$, while the values of $H(x|y)$ increase for $d = 4$ and decrease for $d = 16$. Yet the trend — that the average synchronization values for the healthy controls exceeds those of the MCI subjects which exceeds those of the AD subjects — is preserved. We find for both embedding parameters

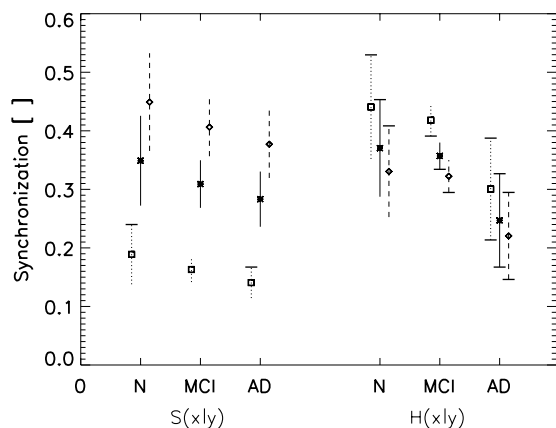
6 *M. A. Kramer et al.*

Fig. 2. The synchronization values $S(x|y)$ and $H(x|y)$ computed for different embedding parameters between electrodes O1 and O2 averaged over the three subject groups: healthy (N), mild cognitive impairment (MCI), and Alzheimer's disease (AD). Here we fix $\tau = 1$ and set $d \in \{4, 10, 16\}$. We indicate the mean values and standard deviations for $d = 4$ by squares and dotted lines, respectively; for $d = 10$ by asterisks and solid lines, respectively; and for $d = 16$ by diamonds and dashed lines, respectively. We indicate statistically significant separations between the healthy and AD subjects, and the MCI and AD subjects in the same way as that used to create Fig. 1.

$d = 4$ and $d = 16$ that the average synchronization values for the healthy subjects exceeds the average synchronization values for the AD subjects. This separation is significant for both $S(x|y)$ and $H(x|y)$ with $d = 4$, and only for $H(x|y)$ with $d = 16$. We indicate this significant separation by drawing a small horizontal line one standard deviation *above* the mean values for the healthy and AD subjects. We note that the separation between the healthy and AD subjects is near significance ($p = 0.09$) for $S(x|y)$ with $d = 16$. As for the $d = 10$ case, the separation between the MCI and AD subjects is statistically significant only for $H(x|y)$. We indicate this significant separation by drawing a small horizontal line one standard deviation *below* the mean values for the MCI and AD subjects. Thus, we may discriminate between the healthy and AD subjects with the synchronization measures $S(x|y)$ and $H(x|y)$, and the MCI and AD subjects with $H(x|y)$ using the embedding parameters $d \in \{4, 10, 16\}$ and $\tau = 1$.

We now perform a similar analysis for the embedding parameter τ . Here we fix $d = 10$ and plot in Fig. 3 the synchronization results for $\tau = 1$ (in asterisks and solid lines — as in Fig. 1,) $\tau = 4$

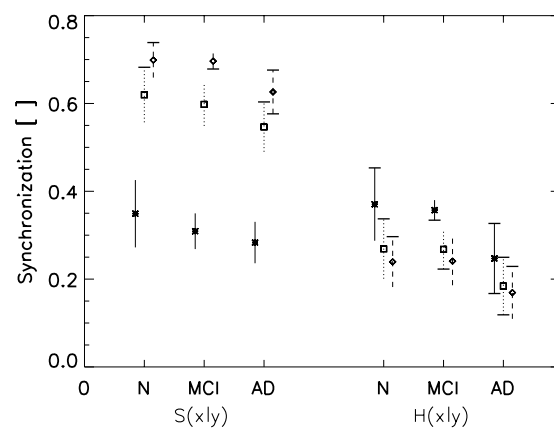


Fig. 3. The synchronization values $S(x|y)$ and $H(x|y)$ computed for different embedding parameters between electrodes O1 and O2 averaged over the three subject groups: healthy (N), mild cognitive impairment (MCI), and Alzheimer's disease (AD). Here we fix $d = 10$ and set $\tau = \{1, 4, 8\}$. We indicate the mean values and standard deviations for $\tau = 1$ by asterisks and solid lines, respectively; for $\tau = 4$ by squares and dotted lines, respectively; and for $\tau = 8$ by diamonds and dashed lines, respectively. We indicate statistically significant separations between the healthy and AD subjects, and the MCI and AD subjects in the same way as that used to create Fig. 1.

(in squares and dotted lines,) and $\tau = 8$ (in diamonds and dashed lines.) We find that, as τ increases, the values of $S(x|y)$ increase and the values of $H(x|y)$ decrease. For $\tau = 4$, the separation between the healthy and AD subjects is significant for both measures, and the separation between the MCI and AD subjects is significant only for $H(x|y)$. For the $\tau = 8$ case, the separation between the healthy and AD subjects is significant for both measures, and the separation between the MCI and AD subjects is significant only for $S(x|y)$. In this case, the $H(x|y)$ result is near significance: $p = 0.06$. We indicate these significant separations following the prescription we use to create Fig. 2. We note that the trend illustrated in Figs. 1 and 2, that the average synchronization values for healthy controls exceeds those for the MCI subjects which exceeds those for the AD subjects, is violated for $\tau = 8$. In this case, the average synchronization values for the MCI subjects exceeds those of the healthy controls. We conclude that the synchronization measures $S(x|y)$ and $H(x|y)$ discriminate between the healthy and AD subjects, and the MCI and AD subjects for d near 10 and τ near 1. In what follows, we fix $d = 10$ and $\tau = 1$.

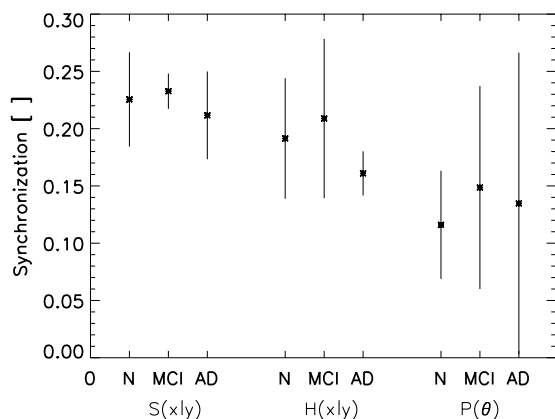


Fig. 4. The synchronization values between electrodes P3 and P4 averaged over the three subject groups: healthy (N), mild cognitive impairment (MCI), and Alzheimer’s disease (AD). We plot the results for the three synchronization measures $S(x|y)$, $H(x|y)$, and $P(\theta)$ from left to right, respectively. For the three measures, we find no statistically significant separations between the three subject groups.

Table 2. The value and standard deviation of the synchronization between electrodes P3 and P4 averaged over subject groups. There are no statistically significant differences.

	$S(x y)$	$H(x y)$	$P(\theta)$
N	0.23 ± 0.04	0.19 ± 0.05	0.12 ± 0.05
MCI	0.23 ± 0.02	0.21 ± 0.07	0.15 ± 0.09
AD	0.21 ± 0.04	0.16 ± 0.02	0.13 ± 0.13

In Fig. 4 we show the synchronization results computed for the EEG data collected at electrodes P3 and P4 (located over the left and right parietal regions, respectively.) We plot these results in the same way as those shown in Fig. 1. For this interhemispheric electrode pair, we find no significant differences in the synchronization results for the three subject conditions. We list the results in Table 2. We find, but do not show, similar results when we compute the synchronization between electrodes: C3 and C4, F3 and F4, and FP1 and FP2. None of these electrode pairs possesses significant differences in coupling between the three subject conditions. We conclude that the only neighboring interhemispheric electrodes with significant synchronization differences between the healthy and AD, and MCI and AD conditions, are electrodes O1 and O2.

5. Discussion

In Sec. 4 we applied three synchronization measures to EEG data collected from three subject groups: healthy controls, patients diagnosed with MCI, and patients diagnosed with AD. We showed that the synchronization between the EEG data recorded at electrodes O1 and O2 decreased for the AD subjects compared to the healthy controls. This decrease was significant for two of the measures — $H(x|y)$ and $P(\theta)$ — and near significance for $S(x|y)$. We computed the $S(x|y)$ and $H(x|y)$ measures with different embedding parameters and showed that the results are robust. Finally, we reported no significant differences in the synchronization values measured at other interhemispheric electrode pairs (e.g., P3 and P4) for the three subject groups.

The methods of analysis we present differ from those used in previous studies of healthy versus AD subjects. Here we employ synchronization measures that operate in the time domain. A common coupling measure for the study of AD is the coherence — a linear measure that operates in the frequency domain. Linear coherence analysis (and some nonlinear synchronization analysis, as in Ref. 16) reveals the coupling between EEG data within different frequency bands. Here, we bandpass filter the EEG time series between 1 Hz and 50 Hz, and apply the three synchronization measures to the data within this wide frequency range. Therefore, we cannot use the synchronization results to determine changes in coupling confined to specific frequency intervals. Instead, we chose to consider the nonlinear coupling between the EEG data throughout a broad frequency band. One may repeat the analysis presented here for data filtered to emphasize other (e.g., more specific) frequency ranges.

We may interpret the results in Sec. 4 in terms of the disconnection model of AD. To do so, we use the synchronization results to infer changes in cortical connectivity. We showed that the synchronization between EEG data recorded at electrodes O1 and O2 decreased significantly for AD subjects compared to healthy controls. We infer from this result a decreased functional connectivity, or disconnection, between the left and right occipital lobes. Such changes in functional connectivity may occur in many ways. At

the cortex, the death of pyramidal neurons and the associated corticocortical connections decreases functional connectivity. In subcortical regions, the loss of white matter decreases functional connectivity. In this study, we infer a disconnection only between the left and right occipital lobes. We do not detect losses in functional connectivity between other interhemispheric regions. This spatial specificity may be due to the experimental conditions because α frequency band activity is more prominent at electrodes O1 and O2 with eyes closed in awake subjects.

We note that the trend of decreased synchronization between electrodes O1 and O2 corresponds to the trend of increased age of the three subject groups. One might therefore attribute the decreased synchronization to normal aging rather than dementia. For example, we find that — assuming the subject ages are drawn from a normal distribution — the separation in the mean ages of the N and AD subjects, and the MCI and AD subjects is statistically significant with $p = 0.042$ and $p = 0.04$, respectively, using the two-sided t -test. (The separation in the mean ages of the N and MCI subjects is not statistically significant, although the power of the test is 0.28.) To determine whether the decreased synchronization results from typical aging or dementia, we will include more (preferably age-matched) subjects in future studies. But, we also note the following: if we exclude the eldest subject from the AD group (age 87), then the mean and standard deviation of the AD subjects becomes 80 ± 5 . For this reduced number of total subjects (of 19 instead of 20), the separation of the mean ages between the N and AD subjects, and the MCI and AD subjects is *nearly* statistically significant ($p = 0.052$ with power 0.79, and $p = 0.057$ with power 0.78, respectively.) We find — but do not show — that the synchronization results are similar for this reduced subject total. For the electrodes O1 and O2, we observe the general trend of decreased synchronization for the N, MCI, and AD groups. The separation between the N and AD subjects, and between the MCI and AD subjects is statistically significant for the measure $H(x|y)$ and near significance between the N and AD subjects for the measure $P(\theta)$. We observe no trend and find no significant separation of the synchronization results for electrodes P3 and P4 in this reduced group of subjects.

The synchronization results we present here do not indicate the anatomical changes associated with decreased interdependence between the left and right occipital lobes. One method to identify these anatomical changes may be a post-mortem examination. Such examinations are the gold-standard for the diagnosis of AD. In this study, no post-mortem examinations were performed. Thus an uncertainty results both in the clinical diagnosis and in the interpretation of the synchronization results. Most studies that distinguish between MCI and AD suffer from this limitation. In the future, synchronization measures combined with traditional linear measures (e.g., power spectra and linear coherence) may provide physicians with additional diagnostic tools perhaps as reliable as the current gold-standard.

Acknowledgments

The authors would like to thank Patricia Case at the Fort Wayne Neurological Center for administrative assistance.

References

1. (2005) Statistics about Alzheimer's disease. [Online]. Available: <http://www.alz.org/>
2. D. S. Knopman, B. F. Boeve and R. C. Petersen, Essentials of the proper diagnosis of mild cognitive impairment, dementia, and major subtypes of dementia, *Mayo Clin Proc* **78** (2003) 1290–1308.
3. R. L. Ernst and J. W. Hay, The US economic and social costs of Alzheimer's disease revisited, *American Journal of Public Health* **84** (1994) 1261–1264.
4. R. P. Brenner, C. F. Reynolds and R. F. Ulrich, Diagnostic efficacy of computerized spectral versus visual EEG analysis in elderly normal, demented and depressed subjects, *Electroencephalogr Clin Neurophysiol* **69** (1988) 110–117.
5. U. Schreiter-Gasser, T. Gasser and P. Ziegler, Quantitative EEG analysis in early onset Alzheimer's disease: A controlled study, *Electroencephalogr Clin Neurophysiol* **86** (1993) 15–22.
6. V. Jelic, P. Julin, M. Shigeta, A. Nordberg, L. Lannfelt, B. Winblad and L. O. Wahlund, Apolipoprotein E epsilon4 allele decreases functional connectivity in Alzheimer's disease as measured by EEG coherence, *J. Neurol. Neurosurg. Psychiatry* **63** (1997) 59–65.
7. C. Besthorn, H. Sattel, C. Geiger-Kabisch, R. Zeffass and H. Forstl, Parameters of EEG

- dimensional complexity in Alzheimer's disease, *Electroencephalogr Clin Neurophysiol* **95** (1995) 84–89.
8. W. S. Pritchard, D. W. Duke, K. L. Coburn, N. C. Moore, K. A. Tucker, M. W. Jann and R. M. Hostetler, EEG-based, neural-net predictive classification of Alzheimer's disease versus control subjects is augmented by non-linear EEG measures, *Electroencephalogr Clin Neurophysiol* **91** (1994) 118–130.
 9. K. O'Connor, J. C. Shaw and C. O. Ongley, The EEG and differential diagnosis in psychogeriatrics, *Br J Psychiatry* **135** (1979) 156–162.
 10. C. Besthorn, H. Forstl, C. Geiger-Kabisch, H. Sattel, T. Gasser and U. Schreiter-Gasser, EEG coherence in Alzheimer disease, *Electroencephalogr Clin Neurophysiol* **90** (1994) 242–245.
 11. G. Adler, S. Brassens and A. Jajcevic, EEG coherence in Alzheimer's dementia, *J. Neural Trans* **110** (2003) 1015–1058.
 12. A. S. Pikovsky, M. G. Rosenblum, G. V. Osipov and J. Kurths, Phase synchronization of chaotic oscillators by external driving, *Physica D* **104** (1997) 219–238.
 13. J. Arnhold, P. Grassberger, K. Lehnertz and C. Elger, A robust method for detecting interdependencies: Application to intracranially recorded EEG, *Physica D* **134** (1999) 419–430.
 14. R. Q. Quiroga, A. Kraskov, T. Kreuz and P. Grassberger, Performance of different synchronization measures in real data: A case study on electroencephalographic signals, *Phys. Rev. E* **65** (2002) 041903.
 15. C. J. Stam and B. W. van Dijk, Synchronization likelihood: An unbiased measure of generalized synchronization in multivariate data sets, *Physica D* **163** (2002) 236–251.
 16. C. J. Stam, Y. van der Made, Y. A. L. Pijenburg and P. Scheltens, EEG synchronization in mild cognitive impairment and Alzheimer's disease, *Acta Neurologica Scandinavica* **2** (2003) 90–96.
 17. P. L. Nunez and R. Srinivasan, *Electric Fields of the Brain* (Oxford University Press, 2006).
 18. W. J. Freeman, Tutorial in neurobiology: From single neurons to brain chaos, *Int. J. of Bif. and Chaos* **2** (1992) 451–482.
 19. T. Schreiber, Interdisciplinary application of nonlinear time series methods, *Phys. Report* **308** (1999) 1–64.
 20. R. Q. Quiroga, A. Kraskov, T. Kreuz and P. Grassberger, Performance of different synchronization measures in real data: A case study on electroencephalographic signals, *Phys. Rev. E* **65** (2002) 041903.
 21. H. Abarbanel, R. Brown, J. Sidorowich and L. Tsimring, The analysis of observed chaotic data in physical systems, *Rev. Mod. Phys.* **65** (1993) 1331.
 22. M. Breakspear, Nonlinear phase desynchronization in human electroencephalographic data, *Hum Brain Mapp* **15** (2002) 175–198.
 23. E. Pereda, R. Q. Quiroga and J. Bhattacharya, Nonlinear multivariate analysis of neurophysiological signals, *Prog Neurobiol* **77**(1–2) (2005) 1–37.